

SUPPORTING INFORMATION

Determination of exosome concentration in solution using surface plasmon resonance spectroscopy

Déborah L. M. Rupert, Cecilia Lässer, Maria Eldh, Stephan Block, Vladimir P. Zhdanov, Jan O.

Lotvall, Marta Bally, Fredrik Höök

Contents

Contents	S2
Mass-uptake determination using SPR	S3
Calibration of the SPR system for protein concentration determination	S3
Size distribution and quantification of biotinylated vesicles performed with NTA	S5
Concentration determination of vesicles using NTA	S6
Lipid mass concentration determined with SPR for different vesicle batches	S6
Determination of total protein content of exosomes	S7
Influence on the concentration determination of the vesicle/exosome size distribution	S8
Vesicle deformation upon adsorption to surface	S10
Exosomes in low salt buffer condition	S16
Materials	S17
References	S18

Mass-uptake determination using SPR

The conditions required to excite surface plasmons depend, among other parameters, on the effective refractive index in close proximity to the surface, n_{film} . For a thin film, the change of this interfacial refractive index be converted into bound mass per surface area¹

$$\Delta\Gamma = d(n_{\text{film}} - n_s)/(dn/dC) \quad (\text{S1})$$

where $\Delta\Gamma$ is the surface coverage, d the effective film thickness, n_s is the refractive index of the solution, and dn/dC is the derivative of the refractive index with respect to the biomolecule concentration in the solution. For an arbitrary film thickness, this sensor response from SPR measurements conducted using Biacore instrumentation can be converted to surface-bound mass $\Delta\Gamma$ as²

$$\Delta\Gamma = \frac{d}{S(dn/dC)[1 - \exp(-d/\delta)]} \Delta RU \quad (\text{S2})$$

where S is the sensitivity in terms of ΔRU per change in bulk refractive index unit, and δ is the decay length of the evanescent field.

Calibration of the SPR system for protein concentration determination

As detailed in the Main Text, the bulk concentration of biomolecules in solution can be determined from the initial rate of signal rate, $\Delta RU/\Delta t$, provided that the measurement is performed under diffusion-limited conditions. In this case, according to Eq. 4 (Main Text), the bulk concentration, C , is proportional to $\Delta RU/\Delta t$, with a proportionality constant $\delta[\xi S'(dn/dC)(D^2 Q)^{1/3}]^{-1}$, where $S' \equiv S \exp(-d_0/\delta)$ determines the reduction in sensitivity induced by the functionalization layer with a thickness d_0 . Since the sensitivity and the accuracy of the flow conditions may vary slightly from instrument to instrument, we made an independent calibration of the measurement system by determining the $\xi S' Q^{1/3}$ product. Such a calibration also makes it possible to compensate for systematic errors in parameters such as temperature, bulk viscosity, decay length, flow handling, *etc.* For this purpose, binding of NeutrAvidin molecules to a sensor functionalized with a biotinylated self-assembled monolayer was investigated. NeutrAvidin was diluted in PBS buffer and concentrations of 27.6 ng/mL and 69 ng/mL were measured using the Pierce bicinchoninic acid (BCA) protein assay kit according to the manufacturer's instructions (Thermo Fisher Scientific, Waltham, MA, USA). Values for

$D_{\text{NeutrAvidin}}$ and $dn/dC_{\text{NeutrAvidin}}$ were taken as $6.10^{-7} \text{ cm}^2 \text{ s}^{-1}$ (reference ³) and $0.19 \text{ cm}^3/\text{g}$ (reference ⁴), respectively.

To verify diffusion-limited conditions, the volumetric flow rate was increased stepwise by a factor 8 (between $5 \text{ }\mu\text{L}/\text{min}$ and $80 \text{ }\mu\text{L}/\text{min}$). The rate of NeutrAvidin adsorption increased by a factor 1.9 ± 0.1 at each step for protein concentrations in the $50 \text{ ng}/\text{mL}$ regime, which confirms operation under diffusion-limited conditions (Fig. S1).

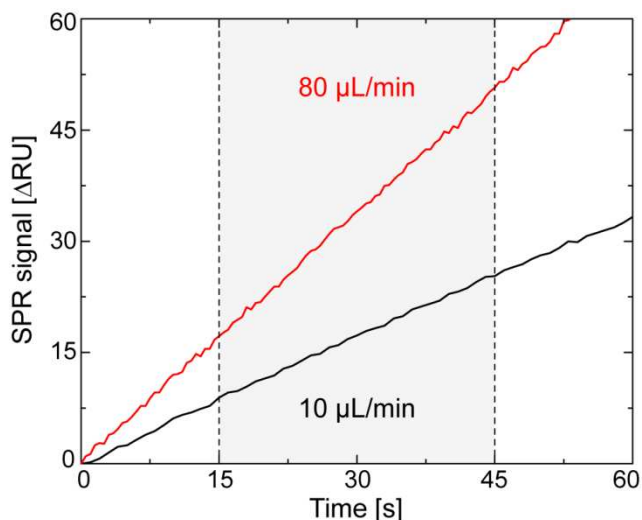


Figure S1. Verification of the diffusion-limited conditions for NeutrAvidin binding to a biotinylated self-assembled monolayer at a concentration of $69 \text{ ng}/\text{mL}$ and at flow rates of $10 \text{ }\mu\text{L}/\text{min}$ (black) and $80 \text{ }\mu\text{L}/\text{min}$ (red). The binding rate is determined from a linear regression fit between 15 and 45 s (grey area).

The so-obtained values for $\xi S' Q^{1/3}$ were $8 \times 10^6 \text{ RU} \times (\text{ms})^{-1/3}$ and $10 \times 10^6 \text{ RU} \times (\text{ms})^{-1/3}$ at flow rates of 5 and $10 \text{ }\mu\text{L}/\text{min}$, respectively. Under the assumption that the volumetric flow rate, Q , was accurately set by the instrument, using $h=0.05 \text{ mm}$, $w=0.5 \text{ mm}$ and $l=2.4 \text{ mm}$ (reference ⁵) and taking into account the reduced sensitivity caused by the 3 nm thin biotinylated self-assembled monolayer, the calibrated sensitivity, S_{cal} , becomes $1.02 \times 10^6 \text{ RU}$ and $1.04 \times 10^6 \text{ RU}$ for flow rates of $5 \text{ }\mu\text{L}/\text{min}$ and $10 \text{ }\mu\text{L}/\text{min}$, respectively. The excellent agreement with the expected S value of $1 \times 10^6 \text{ RU}$ (reference ⁵) validates the rationale behind the use of SPR for determining bulk concentrations of biomolecules. Additionally, this analysis provides an internal calibration of the system for a more accurate determination of the vesicle concentration.

Size distribution and quantification of biotinylated vesicles performed with NTA

Biotinylated vesicles were quantified from three different extrusion batches. Each batch was characterized with NTA in terms of size distribution (Figure S), mean diameter, width at half maximum height and number concentration (see Table S1).

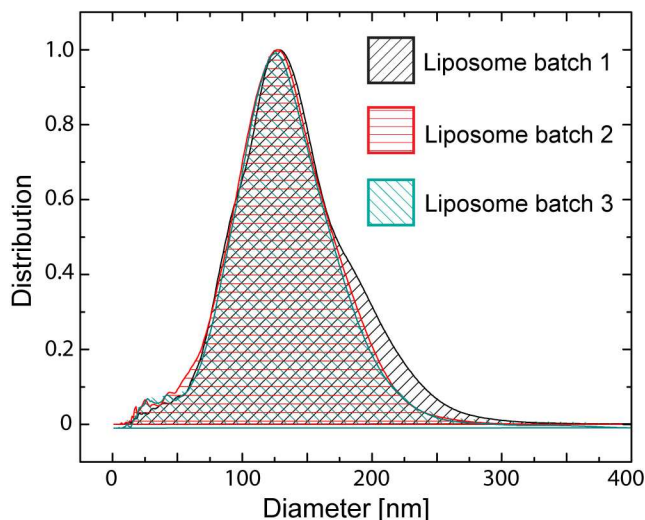


Figure S2. Size distributions of biotinylated liposomes determined with NTA at a lipid mass concentration of 0.5 $\mu\text{g}/\text{mL}$ for the different batches used in this study. The distributions were normalized so that their maxima coincide.

Vesicles	Mean diameter	Half maximum width	Concentration
Batch 1	141 \pm 6 nm	85 \pm 10 nm	4.6 $\times 10^8 \pm 0.9 \times 10^8$ /mL
Batch 2	132 \pm 2 nm	80 \pm 6 nm	7.1 $\times 10^8 \pm 0.8 \times 10^8$ /mL
Batch 3	134 \pm 3 nm	79 \pm 11 nm	5.9 $\times 10^8 \pm 0.4 \times 10^8$ /mL

Table S1. Specification of the size distribution and concentration of biotinylated vesicles from batches 1-3 (with lipid mass concentration of 0.5 $\mu\text{g}/\text{mL}$) according to NTA. The errors

correspond to the standard deviation of four measurements performed on the same sample solution.

Concentration determination of vesicles using NTA

Concentration of liposomes in number per unit volume, $C_{\#}$, can be converted to concentration in mass per unit volume, C_m , as $C_m = C_{\#} \rho \pi h \sum_i \alpha_i d_i^2$, where h (~ 4 nm) is the bilayer thickness, ρ is the bilayer density (~ 1 g/mL) and α_i is the fraction of liposomes with diameter d_i . Liposomes from three different batches (see Figure S and Table S1 for batch characteristics) were quantified with NTA at a lipid concentration of $0.5 \mu\text{g/mL}$.

Vesicles	Stock lipid mass	Concentration measured with NTA	Converted lipid mass
Batch 1	$0.5 \mu\text{g/mL}$	$4.6 \times 10^8 \pm 0.9 \times 10^8 / \text{mL}$	$0.16 \pm 0.04 \mu\text{g/mL}$
Batch 2	$0.5 \mu\text{g/mL}$	$7.1 \times 10^8 \pm 0.8 \times 10^8 / \text{mL}$	$0.20 \pm 0.02 \mu\text{g/mL}$
Batch 3	$0.5 \mu\text{g/mL}$	$5.9 \times 10^8 \pm 0.4 \times 10^8 / \text{mL}$	$0.14 \pm 0.01 \mu\text{g/mL}$

Table S2. Conversion from number concentration to mass concentration for three different batches of vesicles.

Lipid mass concentration determined with SPR for different vesicle batches

The lipid mass concentration was determined with SPR using three different batches of liposomes (Fig. S3).

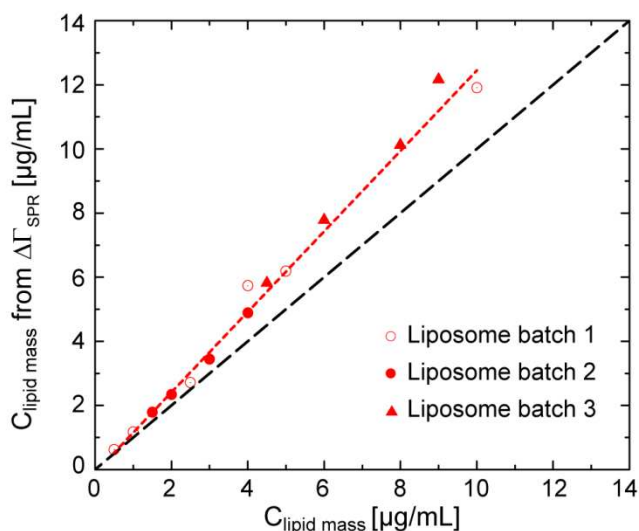


Figure S3. Lipid mass concentration determined with SPR plotted versus injected lipid mass concentration for three different vesicle batches, together with a linear regression fit to the data (dotted line). (The dashed line corresponds to a 1:1 relation between injected and determined lipid concentration.)

Determination of total protein content of exosomes

The determination of total exosomal protein concentration requires a sample preparation step prior to the measurement. Briefly, a small aliquot of HMC-1.2 exosomes was dissolved in PBS, transferred to a new tube, lysed by adding of 20 mM of tris(hydroxymethyl)-aminomethane hydrochloride (Tris-HCl, Aldrich) together with 1% Sodium dodecyl sulfate (SDS, Aldrich) and further sonicated three times for 5 minutes with vortex-mixing in between. The total protein content of the so disrupted exosomal suspension was then quantified using the Pierce bicinchoninic acid (BCA) protein assay kit according to the manufacturer's instructions (Thermo Fisher Scientific, Waltham, MA, USA). The total protein mass concentration of the isolated exosomal solution was determined to be 1.2 ± 0.7 mg/mL.

Influence on the concentration determination of the vesicle/exosome size distribution

The translation of Eqs. S2 and 1 into Eqs. 3 and 6 (see Main Text) is valid for a monodisperse vesicle suspension only. In order to take the relatively broad size distribution of vesicles into account, we use an approach similar to that employed by Jung et al. (reference 2) to describe the contribution of islands to the SPR response. The main idea behind the approach is that the different regions of the size distribution curve contribute additively to the SPR response. In our case with different vesicles, this means that Eq. S2 should be rewritten as

$$S(dn/dC)\sum_i \Delta\Gamma_i \frac{1-\exp(-d_i/\delta)}{d_i} = \Delta RU \quad (\text{S3})$$

where $\Delta\Gamma_i$ is the fractional mass-uptake of sub-populations with a diameter d_i , with

$\sum_i \Delta\Gamma_i = \Delta\Gamma$. To calculate $\Delta\Gamma$ and $\Delta\Gamma_i$, we take into account that under experimental diffusion-limited conditions, the diffusion flux of vesicle subpopulation i , is proportional to $D_i^{2/3}$, where D_i is the corresponding diffusion coefficient. In turn, D_i is proportional to d_i^{-1} (Eq. 5 in Main Text). Thus, the partial diffusion flux is proportional to $d_i^{2/3}$ and the partial surface concentration of vesicles, $C_{\#i}$, is given by

$$C_{\#i}(t) \propto C_{\#} \alpha_i d_i^{-2/3} \Delta t \quad (\text{S4})$$

where $C_{\#}$ is the bulk concentration in number of vesicles per volume and $0 < \alpha_i < 1$ is the vesicle size distribution in solution, with $\sum_i \alpha_i = 1$. Under the assumption that the bilayer density and thickness are independent of vesicle size, the partial and total mass uptakes are accordingly given by

$$\Delta\Gamma_i(t) \propto C_{\#i}(t) d_i^2 \propto C_{\#} \alpha_i d_i^{4/3} \Delta t \quad (\text{S5})$$

$$\Delta\Gamma = \sum_i \Delta\Gamma_i(t) \propto C_{\#} \Delta t \sum_i \alpha_i d_i^{4/3} \quad (\text{S6})$$

Substituting Eq. S5 into Eq. S3 yields

$$C_{\#} \propto \frac{\Delta RU}{\Delta t} \frac{1}{S(dn/dC) \sum_i \alpha_i d_i^{1/3} [1 - \exp(-d_i/\delta)]} \quad (\text{S7})$$

The corresponding bulk concentration expressed in mass per volume, C_m , taking the size distribution into account is then given by

$$C_m = \rho C_{\#} \sum_i \alpha_i v_i \approx \rho h C_{\#} \pi \sum_i \alpha_i d_i^2 \propto \rho h \pi \frac{\Delta RU}{\Delta t} \frac{\sum_i \alpha_i d_i^2}{S(dn/dC) \sum_i \alpha_i d_i^{1/3} [1 - \exp(-d_i/\delta)]} \quad (\text{S8})$$

where ρ and $v_i \approx \pi h d_i^2$ are the lipid bilayer density and volume, respectively.

Hence, the errors originating from a broad size distribution can be characterized by the ratios

$$\frac{\overline{C}_{\#}}{\overline{C}_{\#}} = \overline{d}^{1/3} \frac{[1 - \exp(-\overline{d}/\delta)]}{\sum_i \alpha_i d_i^{1/3} [1 - \exp(-d_i/\delta)]} \quad (\text{S9})$$

and

$$\frac{\overline{C}_m}{\overline{C}_m} = \overline{d}^{-5/3} [1 - \exp(-\overline{d}/\delta)] \frac{\sum_i \alpha_i d_i^2}{\sum_i \alpha_i d_i^{1/3} [1 - \exp(-d_i/\delta)]} \quad (\text{S10})$$

where $\overline{C}_{\#}$ and \overline{C}_m are the number concentration and the mass concentration determined for a sample considered monodisperse with a diameter corresponding to the mean diameter of the size distribution (see Eq. 6 in Main Text).

Using Eqs. S9 and S10, the error induced by assuming a monodisperse suspension of liposomes and exosomes is presented in Table S3. The size distribution was determined with NTA and the bilayer thickness h was assumed to be 4 and 6 nm for liposomes and exosomes, respectively.

Specification of vesicles	$\frac{C_{\#}}{\overline{C}_{\#}}$	$\frac{C_m}{\overline{C}_m}$
----------------------------------	------------------------------------	------------------------------

Biotinylated liposomes:			
mean size:	$\bar{d} = 136 \text{ nm}$	1.02	1.13
bilayer thickness:	$h = 4 \text{ nm}$		
CD63-positive exosomes:			
mean size:	$\bar{d} = 234 \text{ nm}$	1.05	1.21
bilayer thickness:	$h = 6 \text{ nm}$		

Table S3. Concentration determination of biotinylated liposomes and CD63-positive exosomes using SPR: overestimation of the number concentration and the mass concentration using an approximation of a monodisperse sample in comparison to a sample with broad size distribution.

The error induced by assuming a monodisperse suspension of liposomes with an average diameter \bar{d} of 136 nm rather than the true size distribution, d_i , obtained from NTA (see Fig. 1 in Main Text) suggests an underestimation of the number of liposomes and coupled mass of 2% and 13%, respectively. The error induced by assuming a monodisperse suspension containing exosomes with an average diameter \bar{d} of 234 nm rather than the true size distribution, d_i , obtained from NTA (see Fig. 1 in Main Text) suggests an underestimation of the number of particles in exosome solution and coupled mass of 5% and 21%, respectively.

Vesicle deformation upon adsorption to surface

If vesicles of radius r are spherical (Fig. S4a), their contribution to the SPR response is represented as (cf. Eq. S3)

$$\Delta RU_{\text{circ}} \propto 4\pi r^2 [1 - \exp(-2r/\delta)]/2r \quad (\text{S11})$$

where $4\pi r^2$ is the vesicle surface, and $[1 - \exp(-2r/\delta)]/2r$ is the function taking the decrease of the field into account.

If deformed upon adsorption onto a solid substrate, vesicles have the same area as the spherical ones and are represented by a truncated sphere as shown in Fig. S4b, their geometrical parameters, radius ρ and contact radius a ($\in [0, \sqrt{4/3} \cdot r]$) are determined by the following equation

$$\pi a^2 + 2\pi\rho[\rho + (\rho^2 - a^2)^{1/2}] = 4\pi r^2 \quad (\text{S12})$$

and their contribution to the SPR response is represented as

$$\Delta RU_{\text{def}} \propto \pi a^2 / \delta + 2\pi\rho \left(1 - \exp \left\{ - \left[\rho + (\rho^2 - a^2)^{1/2} \right] / \delta \right\} \right). \quad (\text{S13})$$

To solve Eq. S12, let us consider that r and a are given, introduce the dimensionless parameter $p = a / r$, relate a and ρ as

$$a = \rho \sin \phi, \quad (\text{S14})$$

where ϕ is an angle, and rewrite Eq. S12 as

$$p^2 \cdot \left(1 + 2 \frac{1 + \cos \phi}{\sin^2 \phi} \right) = 4. \quad (\text{S15})$$

Taking into account that $\sin \phi = 2 \cdot \sin(\phi/2) \cdot \cos(\phi/2)$ and $\cos \phi = \cos^2(\phi/2) - \sin^2(\phi/2)$, one can rewrite Eq. S15 as

$$p^2 \cdot \left(1 + \frac{1}{\sin^2(\phi/2)} \right) = 4. \quad (\text{S16})$$

This equation yields

$$\phi = 2 \arcsin \left(p / \sqrt{4 - p^2} \right). \quad (\text{S17})$$

Using this expression for ϕ and taking into account that $\sin \phi = 2 \cdot \sin(\phi/2) \cdot \cos(\phi/2)$ and $\cos(\phi/2) = \sqrt{1 - \sin^2(\phi/2)}$ allow to rewrite Eq. S14 as

$$\rho = \frac{a}{2 \cdot \sin(\phi/2) \cdot \sqrt{1 - \sin^2(\phi/2)}}. \quad (\text{S18})$$

Inserting Eq. S17 in S18 finally leads to

$$\frac{\rho}{r} = \frac{4 - p^2}{\sqrt{16 - 8p^2}}, \quad (\text{S19})$$

which allows to express ρ via a .

If further deformed ($p \in [\sqrt{4/3}, \sqrt{2}]$), vesicles have the same area as the spherical ones and are represented by a truncated sphere as shown in Fig. S4c,

$$\pi a^2 + 2\pi\rho \cdot \left[\rho - (\rho^2 - a^2)^{1/2} \right] = 4\pi r^2 \quad (\text{S20})$$

$$\Delta RU_{\text{def}} \propto \pi a^2 / \delta + 2\pi\rho \left(1 - \exp\left\{ -\left[\rho - (\rho^2 - a^2)^{1/2} \right] / \delta \right\} \right) \quad (\text{S21})$$

Eq. S20 can be solved in analogy with Eq. S12. In particular, using again expression S14 and repeating the other steps, one obtains

$$\phi = 2 \arccos\left(p / \sqrt{4 - p^2}\right). \quad (\text{S22})$$

Rewriting Eq. S14 as

$$\rho = \frac{a}{2 \cdot \cos(\phi/2) \cdot \sqrt{1 - \cos^2(\phi/2)}} \quad (\text{S23})$$

leads again to Eq. S19, which is therefore valid for the full, physically meaningful range of $p = a / r$ ($\in [0, \sqrt{2}]$).

Choosing a desirable value of $p = a / r$, obtaining the corresponding value of ρ / r by Eq. S19, and then comparing the responses predicted by Eq. S11 and S13 [or S21], one can identify the influence of vesicle deformation on ΔRU . Fig. S5 gives the expected overestimation of the bulk concentration in dependence of the liposome height after adsorption and shows that a very strong

deformation of liposomes considered monodisperse with a diameter of 136 nm (leading to an almost complete flattening) is necessary to correct for the discrepancy of 50% (see Main Text) observed experimentally. In contrast, a much smaller deformation is needed to correct for a corresponding discrepancy for 240 nm exosomes.

Under the assumption that the vesicle surface coverage is sufficiently small so that the deformed vesicles do not come in contact, it is possible to calculate the maximum overestimation of ΔRU by

$$\max\left(\frac{\Delta RU_{\text{def}}}{\Delta RU_{\text{circ}}}\right) = \frac{2r}{\delta} \cdot \frac{1}{1 - \exp(-2r/\delta)}, \quad (\text{S24})$$

which directly follows from inserting $a_{\text{max}} = \sqrt{2} \cdot r$ into the ratio of Eq. S11 and S13 [or S21]. Hence, if the vesicles are completely deformed upon adsorption, the concentration will be overestimation by +50% and +100% for the 136 nm and the 240 nm exosomes respectively, unless the contraction is included as a correction in the concentration determination.

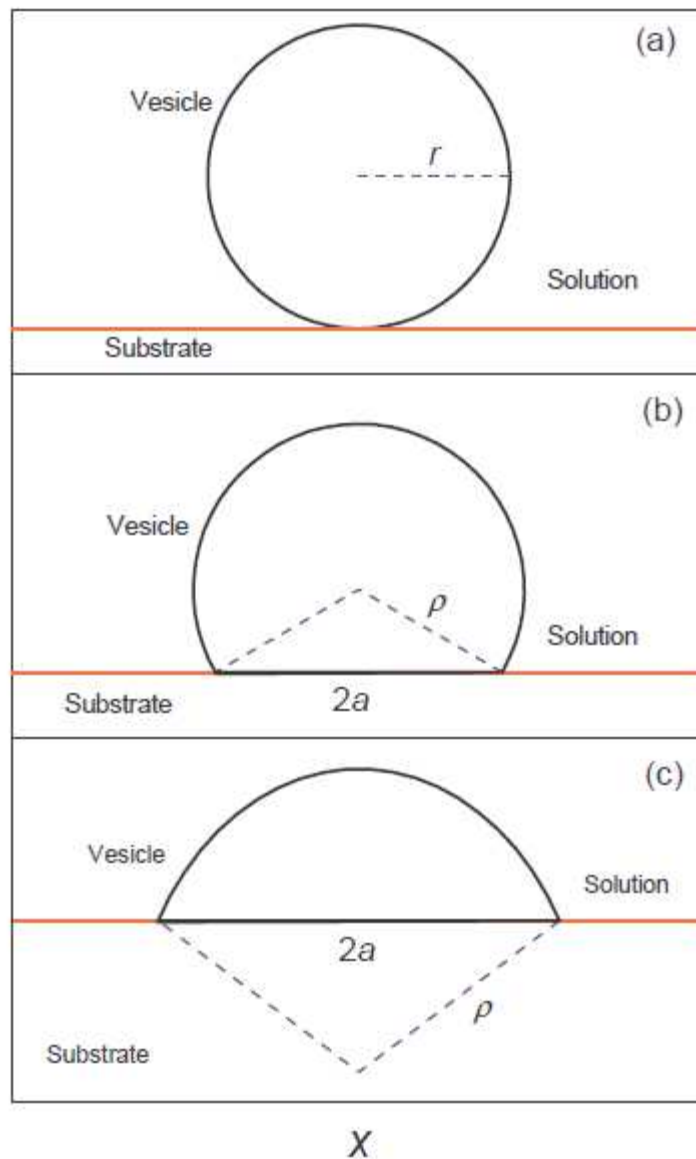


Figure S4: Deformation of a vesicle upon adsorption onto a solid substrate.

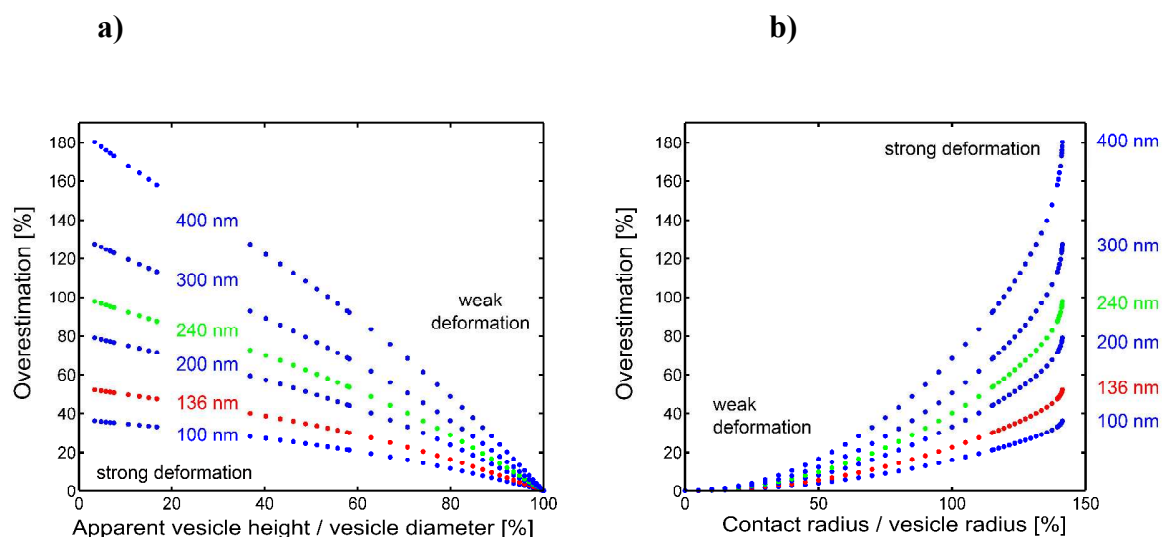


Figure S5. Experimental concentration overestimation for the case that vesicle deformation (occurring during the measurement) is not taken into account during processing of the experimental results. The plots are shown for vesicles with diameters ranging from 100 to 400 nm (indicated in the panels) in a SPR measurement with a decay length of 150 nm: (a) as a function of $h/2r$, and (b) as a function of a/r . An almost complete flattening is necessary to explain the 50% overestimation observed in the experiments performed with liposomes considering they are monodisperse with a diameter of 136 nm (red dots). Due to their larger size, a much smaller deformation of exosomes with a diameter of 240 nm (green dots) is already sufficient to reach the same overestimation.

Exosomes in low salt buffer condition

The number concentration and the size distribution of particles contained in exosome solution were measured with NTA and diluted either in PBS or in TRIS-EDTA at a protein concentration of 2.05 $\mu\text{g}/\text{mL}$. The NTA analysis shows that the exosome number concentration was not affected by the buffer conditions (see Table S4). Also, the two size distributions overlap (see Figure S) and the mean diameter was increased from 216 ± 9 nm in PBS to 240 ± 18 nm in TRIS-EDTA which is expected in low salt buffer conditions (see Table S4).

Buffer condition	Concentration	Mean diameter	Width at half height
PBS	$8.1 \times 10^8 \pm 0.4 \times 10^8 / \text{mL}$	216 ± 9 nm	179 ± 12 nm
TRIS-EDTA	$7.8 \times 10^8 \pm 0.2 \times 10^8 / \text{mL}$	240 ± 18 nm	184 ± 18 nm

Table S4. NTA determination of number concentration and mean diameter of exosome solutions diluted in PBS and in TRIS-EDTA buffer with a protein concentration of 2.05 $\mu\text{g}/\text{mL}$.

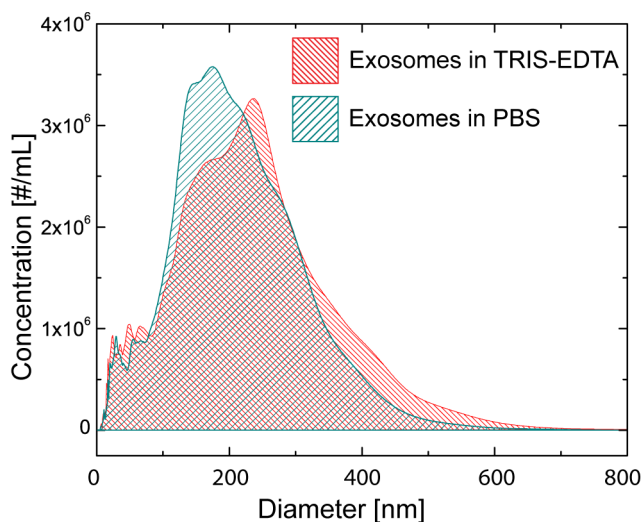


Figure S6. Size distribution of exosome solutions diluted in PBS and in TRIS-EDTA buffer with a protein concentration of 2.05 $\mu\text{g}/\text{mL}$.

Materials

Preparation of biotinylated vesicles. Biotinylated vesicles were prepared by the film hydration and extrusion method. Briefly, a lipid mixture of 1-palmitoyl-2-oleoyl-sn-glycero-3-phosphocholine (POPC) (Polar Avanti lipids, USA) and 1 mol% of 1,2-distearoyl-sn-glycero-3-phosphoethanolamine-N-[biotinyl(polyethylene glycol)-2000] (DSPE-PEG[2000]-biotin) (Polar Avanti Lipids, USA) dissolved in chloroform was dried first under a gentle nitrogen stream and further under vacuum for at least 4 hours. The lipid film was then hydrated by vortexing in Phosphate Buffer Saline (PBS) containing 137 mM NaCl, 2.7 mM KCl and 10 mM phosphate (pH 7.4). The so-obtained vesicle suspension was extruded 13 times through a 50 nm polycarbonate membrane at a pressure of 10 psi. Three individual batches of biotinylated vesicles were prepared and stored at 4°C until use. The lipid mass concentration was determined according to the manufacturer specifications and corresponded to the mass of lipids pipetted from the chloroform lipid solution, dried and further rehydrated in a specific buffer volume.

Exosome production and isolation. Exosomes were isolated from conditioned media from cell cultures of the human mast cell line, HMC-1.2, by differential centrifugation with a filtration step following the protocol previously published by Lässer *et al.*⁶. In brief, HMC-1.2 cells were cultured in a 37°C humidified incubator with 5% CO₂ in Iscove's Modified Dulbecco's Medium supplemented with 10% foetal bovine serum (FBS), 2 mM L-glutamine, 100 units/mL penicillin, 100 µg/mL streptomycin and 1.2 mM alpha-thioglycerol. The FBS was ultracentrifuged at 120 000 × *g* for 18 hours prior to use in the cell cultures, to eliminate contamination of bovine serum extracellular vesicles. Conditional media from HMC-1.2 cells was centrifuged at 300 × *g* for 10 minutes to pellet the cells and cell debris and at 16 500 × *g* for 20 minutes to pellet apoptotic bodies and microvesicles. The supernatant was filtered through 0.2 µm filter (Sarstedt, Nümbrecht-Rommelsdorf, Germany) before being ultracentrifuged in a fixed angle rotor at 120 000 × *g* for 70 minutes to pellet the exosomes. The exosome pellet was finally dissolved in PBS and stored in the -20°C freezer. The buoyant density of exosomes ranging from 1.24 g/mL to 1.31 g/mL was determined by sucrose gradient. These sucrose fractions were identified to contain exosomal RNA (data not shown). Prior to quantification, exosomes were diluted in Tris-EDTA buffer containing 10 mM of tris(hydroxymethyl)aminomethane (Tris, Merck) and 1mM of ethylenediaminetetraacetic acid (EDTA, Sigma).

References

- (1) De Feijter, J. A.; Benjamins, J.; Veer, F. A. *Biopolymers* **1978**, *17*, 1759–1772.
- (2) Jung, L. S.; Campbell, C. T.; Chinowsky, T. M.; Mar, M. N.; Yee, S. S. *Langmuir* **1998**, *14*, 5636–5648.
- (3) Spinke, J.; Liley, M.; Schmitt, F. J.; Guder, H.-.; Angermaier, L.; Knoll, W. *J. Chem. Phys.* **1993**, *99*, 7012–7019.
- (4) Theisen, A.; Johann, C.; Deacon, M. P.; Harding, S. E. *Refractive Increment Data-Book for Polymer and Biomolecular Scientists*; Nottingham.; 2000; p. 64.
- (5) Biacore. *Biacore 2000 instrument handbook*; Biacore AB.; 2001.
- (6) Lässer, C.; Alikhani, V. S.; Ekström, K.; Eldh, M.; Paredes, P. T.; Bossios, A.; Sjöstrand, M.; Gabrielsson, S.; Lötvall, J.; Valadi, H. *J. Transl. Med.* **2011**, *9*, 9.